Macromolecules
ARTICLE

Macromolecules **2010**, *43*, 10283–10290 **10283**
DOI: 10.1021/ma1020424

Ideal Molecular Weight Distributions of Multiblock Copolymers Prepared via RAFT Polymerization

Bastian Ebeling,[†] Martin Eggers,[‡] and Philipp Vana*[,†]

[†]*Institut für Physikalische Chemie, Georg-August-Universität Göttingen, Tammannstr. 6, D-37077 Göttingen, Germany, and* [‡]*Fakultät für Informatik, Technische Universität München, Barer Str. 21, D-80333 München, Germany*

Received September 2, 2010; Revised Manuscript Received October 28, 2010

ABSTRACT: The ideal equilibrium distribution of blocks within multiblock polymers that form when polyfunctional or cyclic reversible addition−fragmentation chain transfer (RAFT) agents are employed in radical polymerization is deduced theoretically. The theory is compared with the actual process via the experimentally determined mass ratio of the two noninterconvertible block types—middle and end blocks—and via the direct fitting of theoretically derived functions to measured size-exclusion chromatography (SEC) curves. Numerical simulations using a statistical approach confirm the results. It is shown that multiblock copolymers of higher homogeneity are prepared with the theoretically examined RAFT strategy than with the commonly used coupling of functionalized prepolymers.

Introduction

Generally, multiblock polymers are linear macromolecules composed of several covalently linked polymer segments. The more special case of multiblock copolymers refers to the case that two different homopolymer segments alternate along such chains.

Multiblock copolymers have gained attention for their ability to form ordered structures when they consist of chemically distinct segments with sufficient length.[1−4] Their most important applications include the use as bulk materials that belong to the class of thermoplastic elastomers, which material properties rest on the effect of microphase separation,[5,6] as compatibilizers[7,8] for blends of immiscible homopolymers, and as pressure-sensitive adhesives.[9,10] There are examples of multiblock copolymers that are known to form responsive polymeric hydrogels, smart materials that have potential applications in drug delivery, tissue engineering, and as chemical and biological sensors.[11−13] Multiblock copolymers with crystallizable segments are the basis of novel semicrystalline materials with promising applications.[14] For many applications, and especially for studying their defined properties, it is generally desired that the multiblock copolymers possess a narrow, well-defined distribution of blocks.

The most common synthesis strategy for multiblock copolymers, one which has already been carried out with a variety of monomer pairs, is the coupling reaction of two different α,ω-functionalized prepolymers. This strategy is universally applicable and relatively easy to implement but carries some fundamental limitations: By step-growth reactions, it is generally very challenging to produce molecules with a high number of blocks. This number, moreover, is difficult to control, and there is a rather large range in the degrees of polymerization of the generated molecules. Assuming equal reactivity of all functional groups, the distribution of blocks among the generated molecules is expressed by the most probable (or Schulz−Flory) distribution.[15,16] Furthermore, because the concentration of reactive chain ends inherently decreases with the chain lengths of the prepolymers, only those with short chains (typically $< 5000\ \mathrm{g\ mol^{-1}}$) can be used for the coupling reaction.

Another common way of producing multiblock copolymers is the alternating addition of two different monomers to a "living" polymerization system, typically via anionic polymerization.[17−19] This method yields multiblock copolymers in which all molecules ideally have the same number of blocks, corresponding directly to the number of subsequently executed polymerization steps. However, this approach entails an enormous experimental effort when high average block numbers are targeted, and impurities and side reactions which deactivate reactive end groups add up with every polymerization step. It has to be noted that in general only a limited number of monomer pairs are suitable for this strategy.

With the advent of controlled radical polymerization techniques, the possibility of producing block copolymers became accessible also for radical polymerization systems. Reversible addition−fragmentation chain transfer (RAFT)[20,21] polymerization is one of the most prominent and, with respect to monomer types and reaction conditions, arguably the most versatile method among them. It proceeds via a degenerative chain transfer mechanism, which induces an equilibrium between propagating macroradicals and dormant polymeric RAFT agents carrying dithio moieties, and has already been successfully employed to produce multiblock copolymers by the previously described method of stepwise monomer addition.[22]

In recent years there has been an increasing number of reports of the synthesis of multiblock copolymers via a new strategy that was pioneered by You et al.[23] and which is illustrated in Scheme 1: When polyfunctional RAFT agents that contain their functional groups along a main chain are employed in a radical polymerization, the resulting macromolecules consist of multiple homogeneous polymer blocks, interconnected by the functional groups of the respective RAFT agent (*multiblock polymer*).[24,25] The subsequent polymerization with another monomer now leads to the formation of multiblock copolymers. Because only two polymerization steps are necessary, this strategy is suitable for all monomer pairs that are amenable to radical polymerization (if employed in the correct order). The RAFT agent's functional

*To whom correspondence should be addressed. E-mail: pvana@uni-goettingen.de.

Published on Web 11/19/2010

Scheme 1. Synthesis of Multiblock Copolymers with Polyfunctional or Cyclic RAFT Agents

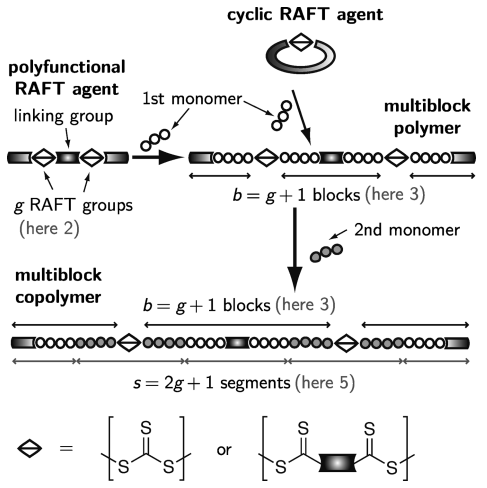

groups will be referred to as *RAFT groups* in this article. Typically, they are of trithiocarbonate type,[26−28] as in our own studies on this topic,[29] but also other groups like bifunctional dithiocarbamates[30−32] can be used. The term "block" is used ambiguously in the literature to describe both polymeric chains between particular functional groups and a part of a polymer chain with homogeneous monomeric composition. To avoid misunderstanding, the former will be denoted *blocks* and the latter *segments* hereafter (see Scheme 1). This appears to be rational because, according to these designations, the number of blocks remains constant within the second polymerization step and can therefore be referred to both multiblock polymers and multiblock copolymers.

As shown in Scheme 1, cyclic RAFT agents can be utilized as well for this strategy.[33−35] This approach differs only in the beginning of the process, when the cyclic RAFT agents are opened up by radicals and form polyfunctional RAFT agents. The subsequent polymerization is basically identical for both cases.[36−39] A limitation of the employment of cyclic RAFT agents instead of polyfunctional ones lies in the fact that the block number of the products can hardly be controlled. Also, the possibility should be mentioned that multiblock polymers with RAFT groups in the main chain are directly prepared by other methods, such as the linking of difunctionalized prepolymers with RAFT groups that are formed within the coupling reaction.[40−42] These polymers can then be used for a RAFT polymerization that corresponds to the second polymerization step in Scheme 1.

Because of the inherent mechanistic characteristics of RAFT polymerization, both the blocks and RAFT groups are constantly redistributed between all individual chains in the polymerization system. Thus, regardless of the initial distribution of the polyfunctional RAFT agent, a well predictable block distribution is expected to occur at the end of the polymerization, owing to this reshuffling process. Despite the notable impact of the described general strategy, there is no information about the expected distribution function available so far. It appears to be useful, however, to know about an ideal function like exists with the Schulz−Flory distribution for the coupling approach. Analytical functions (i) allow for the assessment of control over the polymerization by comparing the dispersity to the ideal value, (ii) they enable the possibility of experimentally determining the average block number in the system, potentially opening up information about the reaction kinetics, and (iii) they allow the evaluation of the quality of the described synthesis strategy for multiblock polymers.

Scheme 2. The Redistribution Mechanism

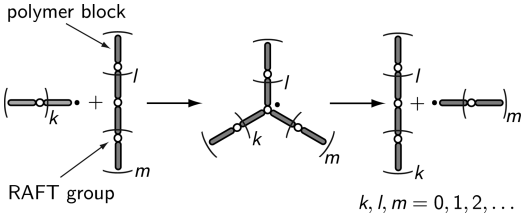

Within this article, a study is presented that was aimed at investigating the above introduced synthesis strategy for multiblock copolymers regarding the expected molar mass distribution of the products.

Redistribution Mechanism

A simplified ideal system is considered here that contains M molecules and only one radical. The average number of blocks $\overline{b}$ per molecule is predefined by the number of functional groups in the employed RAFT agent and remains constant during the polymerization process, assuming that only reactions of the RAFT main equilibrium, namely reversible addition−fragmentation chain transfer and addition of monomer, take place. (Termination and other chain-stopping reactions are neglected as a well-controlled reaction is presumed.) The individual blocks, however, are constantly redistributed in the system according to the repetitive reaction depicted in Scheme 2: The radical attacks one RAFT group of a multiblock polymer and combines with one of the parts of the attacked molecule. The other part is split off as the new growing radical, which attacks another molecule and so on. (The refragmentation to the original products does not alter the system and can therefore be neglected.) After a sufficiently high number of redistribution steps the system will eventually be in equilibrium. The distribution function at equilibrium is represented by N_b, which is the fraction of molecules with b blocks. Obviously, the block distribution prior to the polymerization and the addition of monomer to the radicals do not affect the final distribution of blocks.

It is most practicable to limit all following considerations to the number of blocks b per molecule and its average value $\overline{b}$. In case of the corresponding multiblock copolymers, all formulas can be easily converted to functions of the number of alternating segments s and its average $\overline{s}$ via the equations (see Scheme 1)

$$s = 2b - 1 \quad \text{and} \quad \overline{s} = 2\overline{b} - 1 \tag{1}$$

An open question in the described mechanism, which is of decisive importance for the final distribution, is which of the RAFT groups will be attacked by the radical. In a first approach, two obvious limiting cases exist for this step that are represented by two models. **Model A**: Every RAFT group in the system is attacked with equal probability, independently of the molecule that it belongs to. **Model B**: Every macromolecule is attacked with equal probability. Within the macromolecules, every RAFT group still has an equal chance of being attacked (see Supporting Information, section S1 for further details).

In the following, the block distribution functions N_b will be deduced for both models. It should be noted that the radical could in principle also react with a RAFT group that is part of its own chain, forming a ring. However, formation of rings with higher molar mass is very unlikely to happen as the formation probability decreases with the square of the ring size[43] and has not been reported for systems of the studied type. It is thus not taken into account for the present work but may be considered in a follow-up study.

Physical Interpretation of the Models

The two postulated models A and B can be interpreted physically by hypothesizing that the radical attack on the RAFT groups consists of two elementary steps: **Step 1**: The radical and a random multiblock polymer approach each other via translational diffusion so closely that they can potentially react. They form an encounter pair which, however, can dissociate again without reacting. **Step 2**: Within the encounter pair, the radical attacks a random RAFT group of the attacked polymer molecule, forming a tertiary radical which subsequently reacts to the products. The more RAFT groups in the attacked polymer, the faster is the reaction with this polymer chain. A proportionality of reaction probability and the number of RAFT groups in the attacked polymer is assumed.

It should be noted here that this picture is not in total accordance with the sequence of processes that is generally assumed for reactions of macromolecules, that is, diffusion controlled approach of reactive centers followed by chemically controlled reaction, as e.g. used for kinetic modeling of termination in radical polymerization.[44] According to this latter picture, the term "encounter pair" describes a complex where the two reacting groups have already approached each other, rather than only the two polymer coils, as defined here. This noncompliance is inevitable because of the fact that in the system studied in this work one reagent carries multiple groups that can possibly react, which makes it impossible to totally abstract the diffusion processes from the final reaction step. The here postulated scheme basically accounts for the fact that the effective RAFT agent concentration shows high fluctuations within the system; that is, the concentration of accessible RAFT groups—which governs the reaction probability—is not evenly distributed over the system, as assumed in classical kinetics, but it is much higher during the encounter pair status. This is the reason why the lifetime of the encounter pair in relation to the reaction frequency will affect the selectivity of the process, as described by model A and B, which describe two extreme cases:

- The lifetime of the encounter pair is very short in comparison with the reaction frequency of step 2. Therefore, a high number of encounter pairs are formed prior to every reaction between radicals so that RAFT groups and molecules with more RAFT groups are more likely to react. This case corresponds to model A.
- The lifetime of the encounter pair is very long in comparison with the reaction frequency of step 2. Once formed, every encounter pair will react to the products. Therefore, every macromolecule is attacked with equal probability which corresponds to the definition of model B.

It should be noted that this picture is mainly valid for a system with isolated coils beneath the entanglement limit. With increasing chain length during the controlled polymerization, the RAFT groups will eventually be separated by polymer segments, which reduces the RAFT concentration fluctuations, and chains will mainly occur multiply entangled. Hence, the selectivity of the system will shift toward model A during polymerization. It is for this reason that experiments may well be described by an intermediate situation between model A and B, with the signatures of model A becoming more prominent with increasing chain length and monomer conversion.

Analytical Solution

The distribution functions N_b for both models are deduced pursuing the general strategy to find the functions that fulfill the following condition: At equilibrium, the probability $P_{for}(b)$ of the formation of a molecule with b blocks equals the corresponding probability of dissociation $P_{dis}(b)$ for every value of b:

$$P_{for}(b) = P_{dis}(b) \quad \forall b,\ b = 2, 3, 4, \ldots \tag{2}$$

In order to be able to formulate expressions for the probabilities of formation $P_{for}(b)$ for both models, the auxiliary probability function $P_{fra}(n)$ is introduced that expresses the probability of a radical fragment with n blocks (i) to be the attacking radical, (ii) to combine with the attacking radical within the regarded redistribution step, or (iii) to be formed within this step. Because both parts of the attacked molecule (see Scheme 2) have an equal chance of combining with the incoming radical and every split-off fragment becomes the attacking radical in the subsequent redistribution step, all these three probabilities coincide. Since a new molecule is formed by the combination of two fragments, the probability $P_{for}(b)$ of the formation of a molecule with b blocks can be calculated via the autoconvolution of P_{fra}:

$$P_{for}(b) = (P_{fra} * P_{fra})(b) = \sum_{m=1}^{b} P_{fra}(m) P_{fra}(b-m) \tag{3}$$

When all RAFT groups have an equal chance of being attacked (model A), a normalized value for $P^{A}_{fra}(n)$ can simply be obtained by dividing the number of all possible fragments with n blocks in the system by the total number of possible fragments, which equals the total number of RAFT groups $M(\bar{b} - 1)$. Having in mind that a fragment with n blocks can only be formed by a molecule with at least $b = n + 1$ blocks, because the other fragment must have at least one block, the complete expression can be found to be

$$P^{A}_{fra}(n) = \frac{\sum_{b=n+1} N^{A}_{b}}{M(\bar{b}-1)} \tag{4}$$

For the calculation of $P^{B}_{fra}(n)$ in the case that all molecules have an equal chance of being attacked (model B), it is not sufficient to simply sum up all possible fragments with n blocks. In order to account for the fact that fragments are more likely to be formed by molecules with fewer RAFT groups, every value for N^{B}_{b} must be additionally weighted with the corresponding reciprocal number of RAFT groups $(b - 1)^{-1}$:

$$P^{B}_{fra}(n) = \frac{\sum_{b=n+1} \frac{N^{B}_{b}}{b-1}}{M} \tag{5}$$

Here, the number of molecules M is the normalization factor.

The probabilities of dissociation $P_{dis}(b)$ for the two limiting cases are more straightforward to formulate. If the mechanism holds to model A, $P^{A}_{dis}(b)$ must be proportional to the number of RAFT groups $b - 1$ in the molecules with b blocks and the corresponding existent fraction of molecules N^{A}_{b}. Division by the total number of RAFT groups $M(\bar{b} - 1)$ is needed for normalization:

$$P^{A}_{dis}(b) = \frac{N^{A}_{b}(b-1)}{M(\bar{b}-1)} \tag{6}$$

In case of model B, the probability $P^{B}_{dis}(b)$ that a molecule with b blocks dissociates depends only on the corresponding fraction of molecules N^{B}_{b}, since all molecules are attacked with the same probability. This value is divided by the total number of molecules M to get a normalized formula:

$$P^{B}_{dis}(b) = \frac{N^{B}_{b}}{M} \tag{7}$$

The found expressions (eqs 3, 4, and 6 for model A; eqs 3, 5, and 7 for model B) can now be inserted into the equilibrium condition eq 2. The resulting equations can be solved mathematically to obtain the distribution functions N^{A}_{b} and N^{B}_{b}. A possible

way to do this, involving the conversion of the functions via unilateral *Z*-transform, as well as a more detailed description of the preceding derivations, is shown in detail in the Supporting Information, section S2. The thus found distribution functions are

$$\text{model A:} \qquad \underline{N_b^{\mathrm{A}}} = \frac{1}{\overline{b}-1}\left(\frac{\overline{b}-2}{\overline{b}-1}\right)^{b-2} \tag{8}$$

$$\underline{N_s^{\mathrm{A}}} = \frac{2}{\overline{s}-1}\left(\frac{\overline{s}-3}{\overline{s}-1}\right)^{(s-3)/2} \tag{9}$$

$$\text{model B:} \qquad \underline{N_b^{\mathrm{B}}} = \frac{4}{\overline{b}^2}\left(\frac{\overline{b}-2}{\overline{b}}\right)^{b-2}(b-1) \tag{10}$$

$$\underline{N_s^{\mathrm{B}}} = \frac{16}{(\overline{s}+1)^2}\left(\frac{\overline{s}-3}{\overline{s}+1}\right)^{(s-3)/2}\left(\frac{s-1}{2}\right) \tag{11}$$

where $b = 2, 3, 4, \ldots$ and $s = 3, 5, 7, \ldots$. Equations 9 and 11 were calculated by means of eq 1. The underscores indicate that the functions were normalized by dividing by the total number of molecules M, so that the sum of all function values is 1.

All deduced distribution functions are independent of the number of molecules in the system, though it has to be noted that, strictly speaking, both functions are only valid for infinite numbers of molecules, as the theoretical upper limit for the number of blocks

$$b \le M(\overline{b}-2)+2 \tag{12}$$

was neglected (see Supporting Information, section S2.1). However, the inaccuracy is minimal. Assuming, for example, only 20 molecules with an average block number $\overline{b} = 10$, the sum of function values for b outside of the domain of definition amounts to only approximately 6×10^{-7}% and 7×10^{-13}% for model A and B, respectively. In practice, though, the order of magnitude of M is at least 10^{17}.

The Distribution Functions

Equations 8 and 10 express the ideal distributions of multiblock polymer molecules as functions of the number of blocks b they consist of and of the average block number $\overline{b}$ for both previously described limiting models. Equations 9 and 11 express the distributions as functions of the number of alternating segments for multiblock copolymers. The considerations in the present study were limited to RAFT agents with inherently bifunctional RAFT groups of the type shown in Scheme 1 because the use of these RAFT agents involves a special characteristic that can be used to analyze the kinetics of the actual polymerization process (see below). However, it should be remarked at this point that the derived distribution functions are in principle also valid for polymerization systems where polyfunctional RAFT agents that possess inherently monofunctional RAFT groups, like dithioester groups, along the main chain are employed.

Both deduced distribution functions are plotted for average block number $\overline{b} = 7$ ($\overline{s} = 13$) in Figure 1. The lower x-axis applies to the distributions in dependence on the number of blocks b, while the upper x-axis applies to the distributions in dependence on the number of segments s for multiblock copolymers. It can be seen that distribution function A is strictly decreasing; the maximal value is always at $b_{\max,\mathrm{A}} = 2$. Distribution function B, on the other hand, has a true maximum $b_{\max,\mathrm{B}}$ at

$$b_{\max,\mathrm{B}} = \left(\ln\frac{\overline{b}}{\overline{b}-2}\right)^{-1}+1 \tag{13}$$

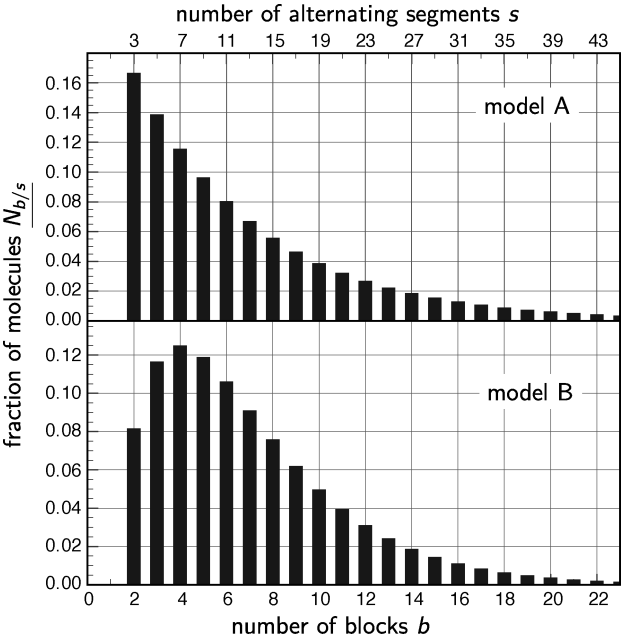

Figure 1. Deduced distribution functions for both limiting models, exemplified shown for $\overline{b} = 7$. The x-axes refer to both plots.

for $\overline{b} > 2e/(e-1)$ (≈ 3.164) (see Supporting Information, section S3.1).

It should be re-emphasized here that a major methodological criterion for a valuable synthesis strategy for multiblock copolymers is that the distribution of segments among the product molecules is as narrow as possible. In this regard, the deduced distribution functions shall be compared with the Schulz−Flory distribution which is the result of the conventional way of preparing multiblock copolymers—the coupling reaction of difunctionalized prepolymers. The broadness of distribution functions is commonly classified by the polydispersity index (PDI): the quotient of number-average molar mass M_{n} and weight-average molar mass M_{w}. Accordingly, M_{n} and M_{w} will express the number weighted and the "block number weighted" number of blocks here. Only if the number of blocks is not proportional to the molar mass is their quotient different to the mass-related PDI.

M_{n} and M_{w} for both distribution functions are calculated in the Supporting Information, sections S3.2 and S3.3. (Although, because of its definition, it was already evident that $\overline{b}$ has to be the result for M_{n} in both cases.) The ideal PDIs of the distribution functions are

$$\mathrm{PDI}^{\mathrm{A}} = \frac{\frac{2(\overline{b}-1)^2}{\overline{b}}+1}{\overline{b}} = \frac{2\overline{b}^2-3\overline{b}+2}{\overline{b}^2} \overset{\text{eq 1}}{=} 2-\frac{6\overline{s}-2}{(\overline{s}+1)^2} \tag{14}$$

$$\mathrm{PDI}^{\mathrm{B}} = \frac{\frac{3}{2}\overline{b}-1}{\overline{b}} = \frac{3}{2}-\frac{1}{\overline{b}} \overset{\text{eq 1}}{=} \frac{3}{2}-\frac{2}{\overline{s}+1} \tag{15}$$

The PDI rises with increasing number of blocks and steadily approaches the values 2 (model A) and 1.5 (model B). An increase of the PDI with higher block number has also been experienced experimentally[29] and does not imply that RAFT agents with more functional groups exert lower control over the polymerization system. It is just what one would expect theoretically on the basis of the present considerations.

In Figure 2, the ideal polydispersity index of multiblock copolymers that were formed according to models A and B is plotted as a function of the average number of alternating

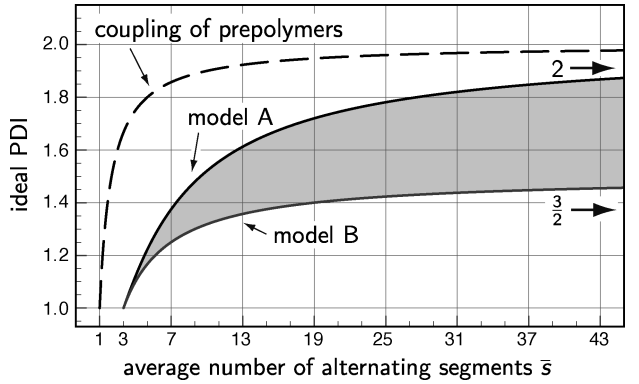

Figure 2. Ideal PDI of multiblock copolymers that were prepared via RAFT polymerization (shaded area) in comparison with the ideal PDI of multiblock copolymers that were prepared by coupling of prepolymers.

segments $\bar{s}$ in the molecules. For comparison reasons, the figure also shows the ideal PDI of multiblock copolymers that were prepared by coupling of difunctionalized prepolymers, i.e., that of the Schulz−Flory distribution ($PDI^{SF} = 2 - 1/\bar{s}$). As the two models A and B represent limiting cases, the ideal PDI of RAFT-prepared multiblock copolymers must lie inside the gray highlighted area. In terms of ideal reactions, the method that is investigated in this article leads consequently to considerably more homogeneous products in terms of chain length dispersity than the conventional coupling method. Furthermore, it is apparent that the PDI of distribution function B is always lower than that of distribution function A. Assuming the mechanism is able to be influenced by the reaction conditions, it would therefore be advantageous to direct it toward limiting model B. On the other hand, the experimentally measured PDI could be regarded as an indicator for the actually occurring mechanism. However, because of deviations from ideal kinetics (e.g., chain-length-dependent reactivity of individual reactions) and constrictions of the measurement method (SEC broadening), experimental PDIs are usually much higher than the ideal values, which makes the extraction of such mechanistic information from PDIs demanding. In the following, two methods will be presented that are clearly better suited for the examination of the occurring mechanism.

Different Sizes of Middle and End Blocks

When polyfunctional RAFT agents with inherently bifunctional groups along the main chain (i.e., of the type shown in Scheme 1) are employed for the synthesis, two different types of blocks can be distinguished that cannot be interconverted into each other during the redistribution process: *end blocks* (two per molecule) that are only connected to one RAFT group at the end of the molecules and *middle blocks* that are connected to RAFT groups on both sides (see Figure 3). The ratio of the total number of middle blocks $\ddot{B}$ and end blocks $\dot{B}$ can be calculated by

$$\frac{\ddot{B}}{\dot{B}} = \frac{\bar{b}}{2} - 1 \tag{16}$$

During the polymerization process, the blocks grow by adding monomer when they are carrying the radical function. Assuming constant addition rate of monomer and constant time spans until the radical fragments react with a molecule, the block masses are proportional to the number of events which release the blocks from an adjoining RAFT group and, thus, to the probability $P_{\mathrm{fra}}(n)$ (see above) that a fragment with n blocks is split off. To obtain a formula for the ratio $r_{\ddot{m}/\dot{m}}$ of the average mass of one individual middle block in comparison with the average mass of one end block, the quotient of the probability for the formation of

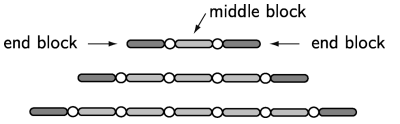

Figure 3. Different block types. For this examplary system, $\ddot{B}/\dot{B} = 9/6 = 3/2$ ($\bar{b} = 5$).

fragments with $n \geq 2$ (a middle block grows) and of the probability for the formation of fragments with $n = 1$ (an end block grows) must be calculated. To account for the fact that for a given probability that a middle or an end block is set free the increase of the average mass is lower when there are more blocks of that type, both expressions have to be divided by the total number of middle and end blocks, respectively:

$$r_{\ddot{m}/\dot{m}} = \frac{\frac{\sum_{n=2} P_{\mathrm{fra}}(n)}{\ddot{B}}}{\frac{P_{\mathrm{fra}}(1)}{\dot{B}}} = \frac{\sum_{n=2} P_{\mathrm{fra}}(n)}{P_{\mathrm{fra}}(1)} \frac{\dot{B}}{\ddot{B}} \tag{17}$$

Insertion of eqs 4 and 16 yields a constant value of $r^{\mathrm{A}}_{\ddot{m}/\dot{m}} = 2$ for pure model A, regardless of the block distribution. In contrast, $r^{\mathrm{B}}_{\ddot{m}/\dot{m}}$ for model B does depend on the actual distribution of blocks. Insertion of eqs 5 and 16 into eq 17 gives

$$r^{\mathrm{B}}_{\ddot{m}/\dot{m}} = \frac{\sum_{b=2} N^{\mathrm{B}}_b \frac{b-2}{b-1}}{\sum_{b=2} \frac{N^{\mathrm{B}}_b}{b-1}} \frac{2}{\bar{b}-2} \tag{18}$$

Depending on the distribution function N^{B}_b, $r^{\mathrm{B}}_{\ddot{m}/\dot{m}}$ can have values ranging from 0 to 2. If it is assumed that the system's equilibration time is short in comparison with the total time of polymerization, the previously deduced equilibrium distribution for model B, eq 10, can be applied. The corresponding result is $r^{\mathrm{B}}_{\ddot{m}/\dot{m}} = 1$ (see Supporting Information, section S4, for calculation and further details).

Thanks to the different ideal values of $r_{\ddot{m}/\dot{m}}$ for the two presumed models, experimentally determined values of $r_{\ddot{m}/\dot{m}}$ can be taken as an indicator for the underlying mechanism. Such data can, e.g., be obtained by cleaving multiblock polymers at the RAFT groups, for example via aminolysis[45] or excess radicals,[46] and subsequently analyzing the products via size-exclusion chromatography (SEC). In our own experiments, which are reported elsewhere[29] (bulk polymerizations of styrene with polytrithiocarbonate, cleavage by aminolysis), the measured ratios were between $r_{\ddot{m}/\dot{m}} \approx 1.65$ and 1.85, which implies that the actual process lies somewhere in between the two limiting cases A and B (but not that the actual process is closer to model B than to model A). It is pleasing to see that the experimental value of $r_{\ddot{m}/\dot{m}}$ lies within the window of theoretically possible values, which indicates that experiments can indeed be described well by the deduced formulas.

In cases that, instead of a distribution of blocks, a mass distribution for the entire multiblock polymers is needed, which can more easily be related to experimental distributions, the distribution function for model A, eq 8, must be corrected with respect to the lower masses of the two end blocks. To this end, a new variable b' is introduced that expresses the number of blocks under the assumption that end blocks contribute only a value of 0.5 to the number of blocks ($b' = b - 1$). The resulting distribution function $N^{\mathrm{A}'}_{b'}$ is then a most probable distribution of b':

$$N^{\mathrm{A}'}_{b'} = \frac{1}{\bar{b}'} \left(\frac{\bar{b}' - 1}{\bar{b}'} \right)^{b'-1} \tag{19}$$

At the same time, the PDI of this function is higher than the PDI that was given above for function A:

$$\mathrm{PDI}^{A'} = 2 - \frac{1}{\bar{b}'} \overset{\text{eq 1}}{=} 2 - \frac{2}{\bar{s}' + 1} \tag{20}$$

If this correction would be applied to the graph in Figure 2, the ideal PDI for model A would rise but still be considerably lower than the PDI for multiblock copolymers that were prepared by the coupling strategy. However, when synthesis strategies for multiblock copolymers are compared, it seems more rational to look at the distribution of the segments instead of the mass distribution.

Consideration of the Mass Distribution of the Individual Blocks

As a final step, the deduced functions for both limiting cases shall be converted into distribution functions of degree of polymerization p. For this purpose, it has to be taken into account that the individual blocks are not fully homogeneous with respect to their chain length. According to the characteristics of ideal living polymerizations, the variation of block masses is generally expressed by a Poisson distribution. Assuming that the monomer addition steps are independent events and neglecting the mass of the employed RAFT agent, the mass distribution of multiblock polymer molecules with the same number of blocks is again a Poisson distribution, whose expected value equates to the sum of expected values of the mass distributions of the individual blocks. This holds true because the Poisson distribution is invariant under convolution (see Supporting Information, section S5.1). The complete chain length distribution is the sum of Poisson distributions for each number of blocks

$$N_p = n \sum_{b=2}^{\infty} \frac{{\nu_p}^p \mathrm{e}^{-\nu_p}}{p!} N_b, \quad p = 1, 2, \ldots \tag{21}$$

where ν_p is the expected value of the degree of polymerization, which can be calculated from the expected value of the degree of polymerization of middle blocks $\ddot{\nu}_p$ for different mass ratios of middle and end blocks $r_{\ddot{m}/\dot{m}}$ by

$$\nu_p = \ddot{\nu}_p \left(b - 2\frac{r_{\ddot{m}/\dot{m}} - 1}{r_{\ddot{m}/\dot{m}}} \right) \tag{22}$$

and where n is the normalization factor

$$n = \sum_{p=1}^{\infty} \sum_{b=2}^{\infty} \frac{{\nu_p}^p \mathrm{e}^{-\nu_p}}{p!} N_b \tag{23}$$

By way of example, Figure 4 shows eq 21 for model B with $\bar{b} = 10$ and $\ddot{\nu}_p = 100$.

Another way to compare the theory with the actual polymerization process is the direct fitting of the calculated distributions to experimentally measured SEC curves of prepared multiblock polymers. For high molecular masses and low numbers of blocks, individual peaks can be resolved for molecules with different block numbers. An experimental SEC curve of multiblock polystyrene prepared in the presence of a polytrithiocarbonate-type RAFT agent is shown in Figure 5 (solid line).[29] The sample was taken at relatively high conversion (47%), and it can be assumed that the system had already reached equilibrium. Obviously, the peaks are still much broader than those of the ideal distribution (as depicted in Figure 4) because of nonideal kinetics and experimental SEC broadening. Only a very simple approach to compensate for this will be included here where the peaks are equally broadened without differentiating between various types of broadening: The Poisson distributions in eq 21 are substituted

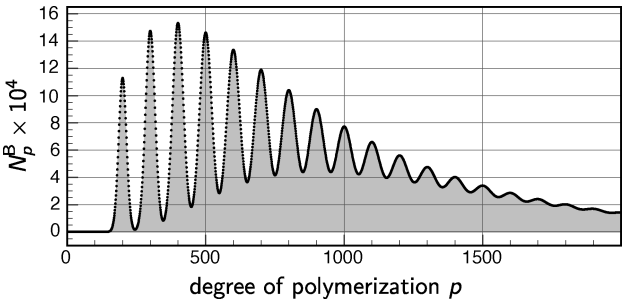

Figure 4. Chain length distribution of multiblock polymers with $\bar{b} = 10$ and $\ddot{\nu}_p = 100$, based on model B.

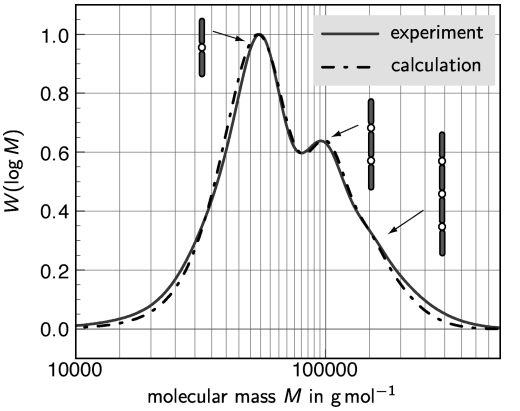

Figure 5. Experimentally measured (bulk polymerization of styrene at 60 °C, mediated by polytrithiocarbonate ($c = 10.5$ mmol L^{-1}) with $\bar{b} \approx 2.3$ and $\ddot{\nu}_p \approx 480$ (47% conversion); for further details see ref 29) and calculated SEC curve (model A, $\bar{b} = 2.3$, $\ddot{\nu}_p = 410$, $H = 55$).

by normal distributions with mean and variance ν_p—an excellent approximation for high values of ν_p—and a broadening factor H is introduced. This one-parametric Gaussian broadening scales the variance of the peaks by H (and therefore the full width at half maximum by $\sqrt{H}$). The resulting distribution $\hat{N}_p$ is

$$\hat{N}_p = \hat{n} \sum_{b=2}^{\infty} \frac{1}{\sqrt{2\pi\nu_p H}} \mathrm{e}^{-[(p-\nu_p)^2]/[2\nu_p H]} N_b, \quad p = 1, 2, \ldots \tag{24}$$

where $\hat{n}$ is the normalization factor

$$\hat{n} = \sum_{p=1}^{\infty} \sum_{b=2}^{\infty} \frac{1}{\sqrt{2\pi\nu_p H}} \mathrm{e}^{-[(p-\nu_p)^2]/[2\nu_p H]} N_b \tag{25}$$

The lower graph in Figure 5 displays the calculated SEC curve that corresponds to eq 24 for model A ($\bar{b} = 2.3$, $\ddot{\nu}_p = 410$, $H = 55$). The fitting parameters are in good agreement with the experimentally obtained data, which are $\bar{b} \approx 2.3$ and $\ddot{\nu}_p \approx 480$. However, with minor modifications to the parameters the experimental SEC curve can be fitted to the function for model B as well. Hence, this fitting method can only be applied to obtain information about the mechanism if very good experimental data for $\bar{b}$ are available.

Numerical Simulation Approach

In order to further verify the deduced analytical equations, a second approach was developed to obtain the ideal distribution functions independently of the previous calculations. The above-described mechanisms A and B were simulated by conducting numerical computations using a self-designed computer program. This program is a script written in MATLAB[47] and is

provided in full within the Supporting Information (section S6.2). Its functions include the statistical simulation of an arbitrary number of reaction steps on a given starting distribution of blocks, applying exactly the above-described mechanistic steps, which for a sufficient number of simulated reaction steps will result in the equilibrium. It is possible not only to simulate the redistribution for the pure limiting models but also to mix the models by defining the ratio in which the two models are randomly applied for the redistribution steps.

Since the simulations can become very time-consuming when using high numbers of molecules and reaction steps, the experiments were simulated repeatedly, averaging the resulting distributions from runs with smaller numbers of molecules to achieve comparable accuracy in less time.

The equilibrium distributions of blocks obtained by simulations for different $\overline{b}$ match exactly the analytical functions that were deduced mathematically and are thus only shown in the Supporting Information (see Figures S6.1 and S6.2). The simulations confirmed also the ideal mass ratio of middle and end blocks $r_{\ddot{m}/\dot{m}}$. The fact that identical results were obtained by the numerical simulations and the mathematical deductions, while both approaches are significantly different from each other, can be regarded as a very convincing proof of their correctness.

In future studies, the simulation script could be employed to analyze the equilibration period of the system as well as the block distributions that result from mixed mechanistic models.

Conclusions

In an attempt to deduce the distribution function of blocks within multiblock polymers, which were prepared employing polyfunctional or cyclic RAFT agents, an idealized polymerization system was considered. Here, the repetitive redistribution step is mechanistically enclosed by two limiting cases regarding the radical attack on the RAFT groups, namely that each RAFT group is attacked with equal probability (model A) or that all molecules have the same chance of being attacked (model B). The equilibrium distribution functions for both models were deduced mathematically. It was found that in terms of the homogeneity of the segment distribution the examined method of using polyfunctional polymeric RAFT agent is superior for the synthesis of multiblock copolymers than the coupling reaction of functionalized prepolymers.

Two methods were presented that allow for the comparison of theory with the actual process. The first method is based on the fact that the end blocks, which cannot be interconverted into middle blocks within the redistribution mechanism, have different chain lenghts for both models: in model A, the end block has only the half size of the middle block, and in model B, end and middle blocks are identical in their length. This difference can be determined experimentally. The second method involves the direct fitting of functions to experimentally measured SEC curves of multiblock polymers with known and low average number of blocks. Preliminary application of these methods to experimental data showed that the actual process most likely lies between the two models, which underlines that the investigated reaction type can be well described by the idealized mechanism. The data available by now, however, were obviously not sufficient to clearly decide by which model the investigated mechanism is better described. In order to even better describe the situation, the existing models could be refined within future work by considering effects like the higher mobility of smaller molecules, the reaction being more likely at the end of chains than in the middle, chain length dependence of addition reactions, and ring formation. Apart from that, it may be assumed that the mechanism depends on the particular reaction conditions. Hence, it can be expected that varying block distributions and mass ratios of middle and end blocks will be observed when similar experiments are conducted under differing conditions, such as different viscosities of the solutions. In this way, even general information about the kinetics of radical polymerization might be attained.

In a parallel approach, numerical simulations of the redistribution process were conducted, which confirmed the correctness of the theoretically deduced results. For future studies, the provided simulation program can be used to investigate systems that are too complex to be treated mathematically or to analyze the time evolution of the distributions.

Acknowledgment. Financial support by the Deutsche Forschungsgemeinschaft (DFG) for the project VA226/5-1 is gratefully acknowledged. P.V. acknowledges receipt of a Heisenberg-Professorship (DFG). We are indebted to Wolfgang Ebeling (University of Hanover) for stimulating ideas regarding the analytical solutions.

Supporting Information Available: Additional explanations, detailed calculations and simulation program. This material is available free of charge via the Internet at http://pubs.acs.org.

References and Notes

(1) Nagata, Y.; Masuda, J.; Noro, A.; Cho, D.; Takano, A.; Matsushita, Y. *Macromolecules* **2005**, *38*, 10220–10225.
(2) Sommerdijk, N. A. J. M.; Holder, S. J.; Hiorns, R. C.; Jones, R. G.; Nolte, R. J. M. *Macromolecules* **2000**, *33*, 8289–8294.
(3) Zhang, Q.; Ye, J.; Lu, Y.; Nie, T.; Xie, D.; Song, Q.; Chen, H.; Zhang, G.; Tang, Y.; Wu, C.; Xie, Z. *Macromolecules* **2008**, *41*, 2228–2234.
(4) Hadjiantoniou, N. A.; Triftaridou, A. I.; Kafouris, D.; Gradzielski, M.; Patrickios, C. S. *Macromolecules* **2009**, *42*, 5492–5498.
(5) Huh, K. M.; Bae, Y. H. *Polymer* **1999**, *40*, 6147–6155.
(6) Lee, D.; Lee, S.-H.; Kim, S.; Char, K.; Park, J. H.; Bae, Y. H. *J. Polym. Sci., Part B: Polym. Phys.* **2003**, *41*, 2365–2374.
(7) Gersappe, D.; Harm, P. K.; Irvine, D.; Balazs, A. C. *Macromolecules* **1994**, *27*, 720–724.
(8) Leclerc, E.; Daoud, M. *Macromolecules* **1997**, *30*, 293–300.
(9) Eastwood, E. A.; Dadmun, M. D. *Macromolecules* **2002**, *35*, 5069–5077.
(10) Eastwood, E.; Viswanathan, S.; O'Brien, C. P.; Kumar, D.; Dadmun, M. D. *Polymer* **2005**, *46*, 3957–3970.
(11) He, C.; Kim, S. W.; Lee, D. S. *J. Controlled Release* **2008**, *127*, 189–207.
(12) Yu, L.; Ding, J. *Chem. Soc. Rev.* **2008**, *37*, 1473–1481.
(13) Rodriguez-Hernandez, J.; Checot, F.; Gnanou, Y.; Lecommandoux, S. *Prog. Polym. Sci.* **2005**, *30*, 691–724.
(14) Gaymans, R. J. *Prog. Polym. Sci.* **2010**, in press.
(15) Schulz, G. V. *Z. Phys. Chem.* (*Leipzig*) **1935**, *B30*, 379.
(16) Flory, P. J. *J. Am. Chem. Soc.* **1936**, *58*, 1877–1885.
(17) Matsushita, Y.; Mogi, Y.; Mukai, H.; Watanabe, J.; Noda, I. *Polymer* **1994**, *35*, 246–249.
(18) Spontak, R. J.; Smith, S. D. *J. Polym. Sci., Part B: Polym. Phys.* **2001**, *39*, 947–955.
(19) Wu, L.; Lodge, T. P.; Bates, F. S. *Macromolecules* **2004**, *37*, 8184–8187.
(20) Chiefari, J.; Chong, Y. K. B.; Ercole, F.; Krstina, J.; Jeffery, J.; Le, T. P. T.; Mayadunne, R. T. A.; Meijs, G. F.; Moad, C. L.; Moad, G.; Rizzardo, E.; Thang, S. H. *Macromolecules* **1998**, *31*, 5559–5562.
(21) Moad, G.; Rizzardo, E.; Thang, S. H. *Aust. J. Chem.* **2005**, *58*, 379–410.
(22) Hadjiantoniou, N. A.; Krasia-Christoforou, T.; Loizou, E.; Porcar, L.; Patrickios, C. S. *Macromolecules* **2010**, *43*, 2713–2720.
(23) You, Y.-Z.; Hong, C.-Y.; Pan, C.-Y. *Chem. Commun.* **2002**, *25*, 2800–2801.
(24) Motokucho, S.; Sudo, A.; Sanda, F.; Endo, T. *Chem. Commun.* **2002**, *17*, 1946–1947.
(25) Motokucho, S.; Sudo, A.; Endo, T. *J. Polym. Sci., Part A: Polym. Chem.* **2006**, *44*, 6324–6331.

(26) Zhou, Y.; Jiang, K.; Song, Q.; Liu, S. *Langmuir* **2007**, *23*, 13076–13084.
(27) Liu, Y.; Cavicchi, K. A. *Macromol. Chem. Phys.* **2009**, *210*, 1647–1653.
(28) Hu, J.; Ge, Z.; Zhou, Y.; Zhang, Y.; Liu, S. *Macromolecules* **2010**, *43*, 5184–5187.
(29) Ebeling, B.; Vana, P. Manuscript in preparation.
(30) Bussels, R.; Bergman-Göttgens, C.; Meuldijk, J.; Koning, C. *Macromolecules* **2004**, *37*, 9299–9301.
(31) Bussels, R.; Koning, C. E. *Tetrahedron* **2005**, *61*, 1167–1174.
(32) Bussels, R.; Bergman-Göttgens, C.; Meuldijk, J.; Koning, C. *Polymer* **2005**, *46*, 8546–8554.
(33) Hong, J.; Wang, Q.; Lin, Y.; Fan, Z. *Macromolecules* **2005**, *38*, 2691–2695.
(34) Wang, Q.; Li, Y.-X.; Hong, J.; Fan, Z.-Q. *Chin. J. Polym. Sci.* **2006**, *24*, 593–597.
(35) Lei, P.; Wang, Q.; Hong, J.; Li, Y. *J. Polym. Sci., Part A: Polym. Chem.* **2006**, *44*, 6600–6606.
(36) Hong, J.; Wang, Q.; Fan, Z. *Macromol. Rapid Commun.* **2006**, *27*, 57–62.
(37) Zhang, L.; Wang, Q.; Lei, P.; Wang, X.; Wang, C.; Cai, L. *J. Polym. Sci., Part A: Polym. Chem.* **2007**, *45*, 2617–2623.
(38) Du, B.; Mei, A.; Yang, Y.; Zhang, Q.; Wang, Q.; Xu, J.; Fan, Z. *Polymer* **2010**, *51*, 3493–3502.
(39) Wu, Y.; Wang, Q. *J. Polym. Sci., Part A: Polym. Chem.* **2010**, *48*, 2425–2429.
(40) Jia, Z.; Xu, X.; Fu, Q.; Huang, J. *J. Polym. Sci., Part A: Polym. Chem.* **2006**, *44*, 6071–6082.
(41) Jia, Z.; Liu, C.; Huang, J. *Polymer* **2006**, *47*, 7615–7620.
(42) Pavlović, D.; Linhardt, J. G.; Künzler, J. F.; Shipp, D. A. *J. Polym. Sci., Part A: Polym. Chem.* **2008**, *46*, 7033–7048.
(43) Wall, F. T.; Hiller, L. A.; Wheeler, D. J. *J. Chem. Phys.* **1954**, *22*, 1036–1041.
(44) D'hooge, D. R.; Reyniers, M.-F.; Marin, G. B. *Macromol. React. Eng.* **2009**, *3*, 185–209.
(45) Qiu, X.-P.; Winnik, F. M. *Macromol. Rapid Commun.* **2006**, *27*, 1648–1653.
(46) Nguyen, D. H.; Wood, M. R.; Zhao, Y.; Perrier, S.; Vana, P. *Macromolecules* **2008**, *41*, 7071–7078.
(47) MATLAB version 7.8.0 (R2009a); The MathWorks, Inc., Natick, MA, 1984−2009.